2-2013

Synthetic controllable turbulence using robust second vorticity confinement

Shengfeng HE
Singapore Management University, shengfenghe@smu.edu.sg

Rynson W. H. LAU

DOI: 10.1111/j.1467-8659.2012.03228.x

COMPUTER GRAPHICS *forum*
Volume 32 (2013), number 1 pp. 27–35

Synthetic Controllable Turbulence Using Robust Second Vorticity Confinement

S. He and R. W. H. Lau

Department of Computer Science, City University of Hong Kong, Hong Kong
shengfeng_he@yahoo.com,rynson.lau@cityu.edu.hk

Abstract

Capturing fine details of turbulence on a coarse grid is one of the main tasks in real-time fluid simulation. Existing methods for doing this have various limitations. In this paper, we propose a new turbulence method that uses a refined second vorticity confinement method, referred to as robust second vorticity confinement, and a synthesis scheme to create highly turbulent effects from coarse grid. The new technique is sufficiently stable to efficiently produce highly turbulent flows, while allowing intuitive control of vortical structures. Second vorticity confinement captures and defines the vortical features of turbulence on a coarse grid. However, due to the stability problem, it cannot be used to produce highly turbulent flows. In this work, we propose a robust formulation to improve the stability problem by making the positive diffusion term to vary with helicity adaptively. In addition, we also employ our new method to procedurally synthesize the high-resolution flow fields. As shown in our results, this approach produces stable high-resolution turbulence very efficiently.

Keywords: turbulence, smoke simulation, vorticity confinement, physically-based modeling

ACM CCS: I.3.7 [Computer Graphics]: Three-Dimensional Graphics and Realism-Animation I.6.8 [Simulation and Modelling]: Types of Simulation-Animation

1. Introduction

Fine details of turbulence are important in synthesizing realistic fluid flows. However, they are computationally expensive to produce due to the need to represent turbulent behaviours in high-resolution grids. Although a number of methods have been proposed to capture fine details to produce visually interesting appearances on low-resolution grids, they have high computation complexity and do not support real-time simulation. Thin vortical features are a significant factor to represent highly turbulent flows, but they are also difficult to capture with most existing methods.

In this paper, we propose a new approach that creates highly turbulent effects on a coarse grid, and allows intuitive control of turbulent motion by altering vortical region size and timescale. The main method of our approach is based on second vorticity confinement (VC2) proposed by Steinhoff *et al.* [SFWD03]. VC2 is a new version of the popular method, vorticity confinement (VC1) [SU94, FSJ01]. VC2 improves the original method. As it satisfies the momentum conservation laws, it can capture thin vortices more accurately. In addition, VC2 includes a positive diffusion term, together with a negative diffusion term to *define* vortical structures by intuitive parameters. This method specifically treats vortical structures with a controlled 'model' structure directly on the grid.

There is a stable condition for VC2: the pair of confinement terms, positive and negative diffusion terms, must be balanced. However, the confinement strength during the stable condition is insufficient to produce highly turbulent flows. In this paper, we propose a robust formulation (robust VC2 (RVC2)) to widen the stable condition of VC2, making it sufficiently stable for high confinement strength situation, while keeping the original advantages. This is achieved by varying the positive diffusion with helicity. This modification is equivalent to adding an adaptive constraint to the total confinement, and helps maintain the balance of the two terms.

High-resolution fluid simulation usually contains a great deal of fine details. In order to achieve high-resolution simulation with low computational cost, we procedurally synthesize a vector field in high resolution by our RVC2. This vector field is stable since it is perfectly balanced. This greatly reduces the computation complexity of the method, and at the same time produces highly turbulent details

without any unrealistic effects. To accelerate our method further, we have implemented our method on GPU.

In summary, our main contribution of this work is a new approach that combines our robust VC2 (RVC2) with a synthesis scheme for generating turbulence. The new method is robust, intuitive to control and efficient. While RVC2 helps produce highly turbulent flows, the synthesis scheme helps synthesize high-resolution flows efficiently without causing artefacts. Our turbulence approach is also easy to implement since it is a fully grid-based method, and is able to generate high-resolution turbulent flows in real time.

The rest of this paper is organized as follows. Section 2 gives a brief overview of related works. Section 3 presents our turbulence method, which is based on VC2, our new formulation and a synthesis scheme. Section 4 discusses some experimental results. Finally, Section 5 briefly concludes this work and discusses possible future work.

2. Related Work

Fluid simulation in computer graphics is typically governed by the incompressible Navier–Stokes (N-S) equations:

$$\frac{\partial \mathbf{u}}{\partial t} = -(\mathbf{u}\cdot\nabla)\mathbf{u} - \frac{1}{\rho}\nabla p + \mu\nabla^2\mathbf{u} + \boldsymbol{f}, \tag{1}$$

$$\nabla\cdot\mathbf{u} = 0, \tag{2}$$

where $\mathbf{u}$ is the velocity, p is the pressure, ρ is the mass density, μ is the diffusion coefficient and $\boldsymbol{f}$ is the external force. Readers may refer to [Bri08] for details of the numerical methods for solving the incompressible N-S equations. For the sake of efficiency and visual appearance, fluid is usually assumed to be inviscid in computer graphics [YKH*09, HWPW11, LAF11]. This means that the third term on the right-hand side of Equation (1), which is the diffusion term, is ignored. On the contrary, this diffusion term is a key element in our method to achieve robustness and intuitive control, as will be described in Section 3.

There are works to produce fluid flows with visually interesting appearances. The semi-Lagrangian advection method is an unconditionally stable method [Sta99]. Although this method allows large time steps, it suffers from numerical dissipation. Reducing numerical dissipation helps produce more accurate fluid flow behaviour. High-order numerical schemes have been proposed to address this problem, including BFECC [KLLR07], MacCormack method [SFK*08], fully conservative semi-Lagrangian method [LAF11] and other advection methods like hybrid particle/grid approach fluid-implicit particles (FLIP) [ZB05]. Although these high-order numerical schemes are more accurate, they still cannot capture fine details on a coarse grid. One major problem with capturing turbulent details is scalability in real-time applications.

Noise integration is a practical solution for producing turbulence effects. Kim *et al.* [KTJG08] introduce wavelet noise to generate fine turbulence details. Schechter and Bridson [SB08] use a simple linear model and add turbulence details with flow noise to an up-sampled simulation. Narain *et al.* [NSCL08] use a procedural method based on the energy cascade theory to add turbulence. Particles with frequency matched curl noise [PTC*10] and random forcing [CZY11] are also used to enhance turbulence simulations. Although these noise-based methods produce good small-scale details, they need extra efforts to maintain the large-scale behaviour temporally consistent.

Another solution for capturing turbulent details is to re-inject the energy dissipation back to the fluid flows. To capture more small-scale rolling details on a coarse grid, vorticity confinement (VC1) [SU94, FSJ01] is a popular method for generating turbulence effects at low computational cost. However, it only approximately conserves momentum, and a high confinement strength prevents the fluid flows from rising properly as shown in the middle and right diagrams of Figure 3a, which have also been pointed out by Selle *et al.* [SRF05]. Some works propose to modify the formulation to address the drawback of VC1 [Rob04, HWPW11]. However, these methods are unstable and the simulation will blow up if a high coefficient is set. Selle *et al.* [SRF05] propose a simplified vortex particle method to combine grid-based and particle-based methods. This method can also be considered as localized VC1. Vortex particles are required to be seeded carefully to avoid unnatural rotation. Yoon *et al.* [YKH*09] procedurally synthesize the vector field by the vortex particle method to improve sub-grid visual details. Pfaff *et al.* [PTSG09] seed the vortex particles randomly at pre-computed artificial boundary layers to represent anisotropic effects near obstacles. In general, most of these existing turbulence methods have difficulty in controlling the behaviour of turbulent flows. It is difficult to adjust the parameters to achieve the desired visual effects.

Steinhoff *et al.* improve their vorticity confinement method [SU94] by proposing VC2 [SFWD03]. They show that VC2 can also be extended to solve the wave equations on Eulerian grids [SC10]. Comparing with VC1, which only approximately conserves momentum, VC2 exactly conserves momentum and captures small-scale features more accurately. A detailed investigation [Cos08] shows that VC2 is able to produce less dissipation as a high-order numerical scheme. However, due to the stability problem, VC2 cannot be used to produce highly turbulent effects. In summary, most existing methods either suffer from the stability problem or are computationally too expensive for simulating highly turbulent flows at interactive frame rates.

3. Turbulent Flow Simulation

Highly turbulent flows usually contain a large amount of thin vortical structures, which are required to represent chaotic effects. VC2 is proposed to capture vortical features. However, due to the stability problem, VC2 is unable to keep vortical structures thin. In this section, we first briefly summarize VC2 in Section 3.1, and then present our new robust method in Section 3.2 and our high-resolution turbulence synthesis approach in Section 3.3. In the rest of this paper, symbols printed in bold denote vectors, and those printed in non-bold denote scalars.

3.1. Second vorticity confinement

VC2 is proposed by Steinhoff *et al.* [SFWD03] to improve the original vorticity confinement (VC1) [SU94]. VC2 is proposed with three goals to address the drawbacks of VC1:

(i) To explicitly conserve momentum.
(ii) To prevent thin vortical structures from becoming too large or too thin.
(iii) To achieve nonlinearity. A linear combination of terms in the derivatives cannot lead to a stable confinement for any finite range of coefficients. It would only result in divergence.

To satisfy the second goal, VC2 includes the viscous force (or positive diffusion), together with a contraction term (or negative diffusion) to define the vortical structures. Hence, the confinement term, $\boldsymbol{f}_{conf}$, is constructed by two terms as:

$$\boldsymbol{f}_{conf} = \mu\nabla^2\mathbf{u} + \mathbf{s}, \tag{3}$$

where $\mu\nabla^2\mathbf{u}$ is the positive diffusion term and $\mathbf{s}$ is the negative diffusion term defined as:

$$\mathbf{s} = \nabla \times \mathbf{m}, \tag{4}$$

where $\mathbf{m}$ is the harmonic mean of the local vorticity stencil, which is the sum of $(N-1)$ neighbour nodes together with the central node:

$$\mathbf{m} = \frac{\boldsymbol{\omega}}{\tilde{\boldsymbol{\omega}}}\left[\frac{\sum_l(\tilde{\boldsymbol{\omega}}_l)^{-1}}{N}\right]^{-1}, \tag{5}$$

where

$$\tilde{\boldsymbol{\omega}} = |\boldsymbol{\omega}| + \delta. \tag{6}$$

Here, $\tilde{\boldsymbol{\omega}}$ is a non-zero absolute value of $\boldsymbol{\omega}$ and δ is a small positive value to avoid division-by-zero. Note that although we use harmonic mean in this formulation, other forms can also be used as long as they give a large weight to a grid point with a small value.

For $\nabla \cdot \mathbf{u} = 0$ and $\boldsymbol{\omega} = \nabla \times \mathbf{u}$, Equation (3) can be written as

$$\boldsymbol{f}_{conf} = -h\nabla \times (\mu\boldsymbol{\omega} - \epsilon\mathbf{m}), \tag{7}$$

where h is the grid size and μ and ϵ are the positive and negative diffusion coefficients, respectively, that control the size and timescale of the vortical regions.

Equation (7) satisfies all three goals. First, it explicitly conserves momentum since the same difference operator acts on $\boldsymbol{\omega}$ and $\mathbf{m}$, causing the confinement terms to produce equal amount of linear momentum in each direction. Second, the positive diffusion term helps stabilize the confinement, and the negative diffusion term helps contract and relax the vortical structures to a fixed shape. Third, the negative diffusion term is a nonlinear term. The vorticity cannot diverge since the negative diffusion term is a local term so that the total vorticity is conserved in a vortical region.

3.2. Robust formulation

VC2 is a more accurate and intuitive method than VC1. The pair of confinement terms together help create thin vortical structures. Stable solutions can be produced when the two terms are approximately balanced. Since VC2 involves second derivatives of velocity, it is not as robust as VC1, which involves only first derivatives. As demonstrated by Fan *et al.* [FWD*02], the value of ϵ/μ must be less than 5 in order to satisfy the stable condition. However, the confinement strength under the stable condition is not sufficient to produce highly turbulent flows. Although sub-stepping [LM91] may be used to improve stability, it is unable to locally balance the confinement. As a result, it still cannot produce highly turbulent flows.

To address this problem, we propose a robust formulation for VC2, referred to as RVC2. We note that VC2 is unstable because as the negative diffusion term increases, the total confinement becomes out of balance. However, the negative diffusion term must increase in order to upgrade the turbulent level. Our idea here is to adaptively adjust the positive diffusion term so that it is able to balance the negative diffusion term adaptively. In other words, the vortical structures that are too thin will be restricted, and the structures that too large will be contracted more significantly. This is equivalent to adding an adaptive constraint on the total confinement term, $\boldsymbol{f}_{conf}$, to make it stable. Inspired by [Rob04], we adopt the concept of *helicity* here as a constraint in the positive diffusion term. Helicity is defined as $\mathbf{u} \cdot \boldsymbol{\omega}$, which is a vortex indicator. High helicity values indicate the locations of the vortex regions. Involving the helicity in the positive diffusion term may help balance the vortex regions. We introduce $\frac{|\mathbf{u}\cdot\boldsymbol{\omega}|}{|\boldsymbol{\omega}|}$ as a scaling factor to Equation (7), allowing the helicity to control the magnitude of the positive diffusion term. The final formulation of the RVC2 is defined as follows:

$$\boldsymbol{f}_{conf} = -h\nabla \times \left(\mu|\mathbf{u}\cdot\boldsymbol{\omega}|\frac{\boldsymbol{\omega}}{|\boldsymbol{\omega}|} - \epsilon\mathbf{m}\right). \tag{8}$$

The positive diffusion term now varies with helicity. It maintains the confinement strength adaptively, whatever the negative diffusion coefficient is set. The positive diffusion term keeps the total confinement within a stable state. An important feature of our robust approach is that it also explicitly conserves momentum, as a spatial derivative operator is still involved in front of the modified confinement term.

Our method treats vortical structures with a controlled 'model' structure directly on the grid, and the vortical structures are *defined* by the confinement method. Thus, small-scale features can be intuitively controlled by the positive diffusion term (acting like spreading) and the negative diffusion term (acting like contracting). In addition, our modification maintains the spreading behaviour and varies its degree adaptively. In our method, the values of ϵ/μ can be set as high as 300 (vs. 5 in VC2), as demonstrated by our experiments shown in Section 4.

Note that when two neighbour vortices have approximately opposite vorticity directions, it will cause oscillation. This oscillation will prevent the flows from properly rising. We have implemented a simple rule to avoid this problem. For the negative diffusion term, if the scalar product of any of the vorticity vectors in the local stencil with the central node is negative, $\mathbf{m}$ is set to zero. In our experiments, this simple rule is indispensable to the stability of the simulation.

3.3. Synthesis of turbulence details

To achieve a high-resolution fluid simulation with extensive small-scale details but low computation time, we procedurally synthesize high-resolution turbulent details and combine them to a up-sampled high-resolution simulation. This approach is able to avoid solving the N-S equations on high-resolution grid, which is computationally very expensive. It is also able to maintain sub-grid turbulence.

First, we solve the N-S equations and apply our RVC2 on a coarse grid. We then up-sample the coarse velocity field to get a

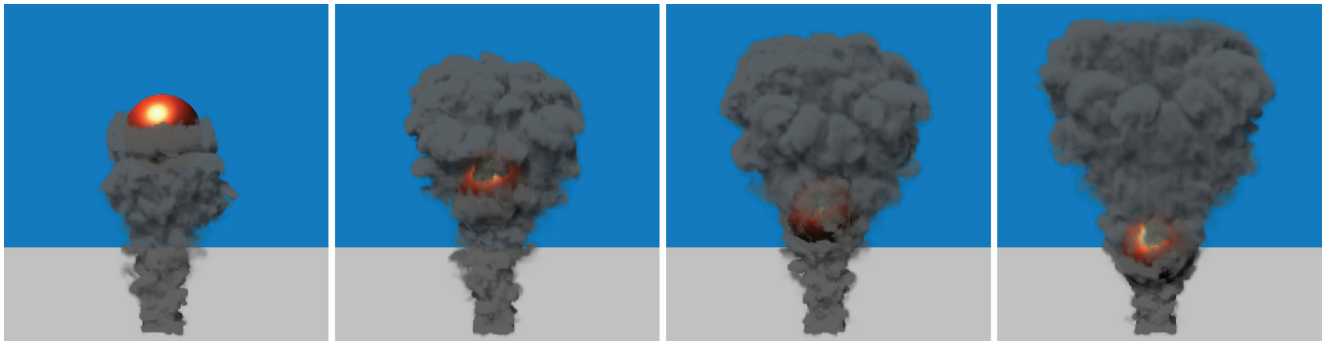

Figure 1: *An animation sequence of a highly turbulent smoke flowing around a moving sphere. It is a* $128 \times 128 \times 128$ *simulation (with* $\epsilon_{low} = 2.0$, $\mu_{low} = 0.03$, $\epsilon_{high} = 4.0$ and $\mu_{high} = 0.02$*) with a* $64 \times 64 \times 64$ *coarse grid, at 37.7 frames per second on average.*

high-resolution simulation. Based on this high-resolution simulation, we employ our RVC2 once again to synthesize a vector field. This high-resolution vector field contains extensive sub-grid turbulence as it is generated from a high-resolution simulation. Finally, we combine the velocity field with the synthesized vector field as the final flow field to advect the density. The pseudo-code of a simulation step with our simulation method is shown in Algorithm 1. We use cubic B-spline interpolation to up-sample the coarse grid, which is able to produce less dissipation during the up-sampling process.

Algorithm 1. A simulation step of our simulation method

1: // Computing the low resolution turbulence
2: Velocity $\mathbf{u}_{low}$ advection with the MacCormack method
3: Apply Robust Second Vorticity Confinement (RVC2)
4: Pressure projection with Poisson solver
5:
6: // Computing the high resolution details
7: Up-sample $\mathbf{u}_{low}$ to $\mathbf{u}_{high}$
8: Synthesize the vector field $\mathbf{v}_{high}$ by RVC2 based on $\mathbf{u}_{high}$
9: $\mathbf{u}_{high} + \mathbf{v}_{high}$ to get final high resolution velocity field
10: Density advection with the MacCormack method
11: Render density by ray-marching

In our approach, RVC2 is applied on a coarse grid and involved in the governing equations. Hence, it affects the behaviour of the main flows. On the other hand, we do not down-sample the combined velocity to the next time step, as down-sampling is also computational expensive. This means that the combined velocity is only used in the density advection stage. Thus, the synthesized vector field is able to make the density field more chaotic and generate sub-grid turbulence.

Another important feature of our synthesis method is that the high-resolution vector field is surprisingly stable as the positive diffusion term is involved. This is different from other confinement synthesis methods such as [YKH*09, HWPW11], which synthesize the high-resolution vector field by a confinement method (vortex particle or vorticity confinement) and involve the negative diffusion term only. The vector field that they synthesize becomes unstable once the confinement strength reaches a certain degree. However, since the positive diffusion term is also involved in our approach, the vector field that we synthesize is perfectly balanced. The confinement range is much wider. Hence, when applied with RVC2 on a coarse grid, our approach is able to intuitively produce highly turbulent flows. In low resolution, ϵ_{low} and μ_{low} define the vortical region size and the timescale, respectively. In high resolution, ϵ_{high} and μ_{high} control the sub-grid turbulence. As a result, our approach can be controlled by four intuitive parameters, two in low resolution and two in high resolution, to obtain the desired visual appearance.

4. Results and Discussion

In this section, we present and discuss a number of experiments to demonstrate the performance of our turbulence method. All these experiments were performed on a PC with an Intel Core i7 CPU, 6GB RAM and NVIDIA GeForce GTX 580 graphics card. Both the solver and the renderer are implemented in CUDA running entirely on the GPU. We have implemented an Eulerian fluid smoke simulator, and applied Jacobi iteration for solving the Poisson equation. A stable MacCormack method [SFK*08] is used as the advection approach. To balance between visual effect and performance, ray-marching is used in our implementation to produce self-shadow of the smoke. We set the stencil size of the harmonic mean N to 7, which optimizes between performance and visual quality. (We have found that while increasing N further will lead to a higher computational cost, it does not have a significant effect on the visual quality.) In addition, *no-stick* boundary condition is used in our experiments.

Figures 1 and 2 show some highly turbulent smoke colliding with a moving sphere and a static sphere, respectively. The smoke here is ultra turbulent, having a higher density and moving at a higher speed than the other simulations shown in this paper. These two animation sequences show that our method is robust enough to produce highly turbulent effects. Figure 2 is produced from a high-resolution simulation of $256 \times 256 \times 256$. It shows extensive turbulence details.

Figure 3 compares the robustness of our method with two existing energy injection methods: VC1 [SU94, FSJ01] and VC2 [SFWD03]. The confinement strength is set from low (left diagrams) to high (right diagrams). We can see that under a high confinement strength, VC1 is not able to rise properly and VC2 suffers from the narrow range of stable condition. On the other hand, our method can produce a proper turbulence even when ϵ/μ is set to 300 as shown in

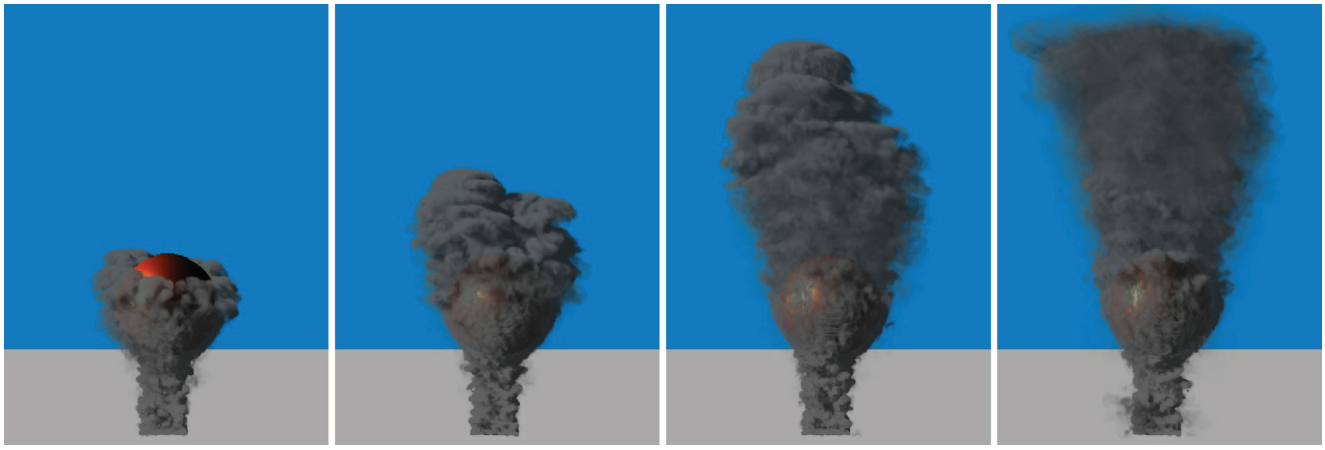

Figure 2: *An animation sequence of highly turbulent smoke flowing around a static sphere. It is a* $256 \times 256 \times 256$ *simulation* (*with* $\epsilon_{low} = 0.65$, $\mu_{low} = 0.02$, $\epsilon_{high} = 3.6$ *and* $\mu_{high} = 0.038$) *based on a* $128 \times 128 \times 128$ *coarse grid, at 6.5 frames per second*.

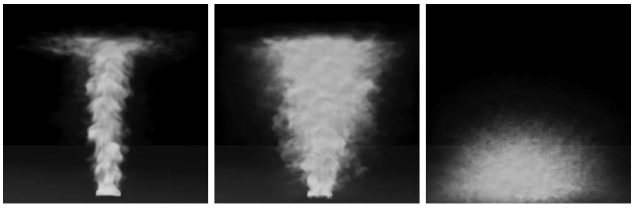

(a) Vorticity Confinement, ε is: 0.25, 0.5, 2.0

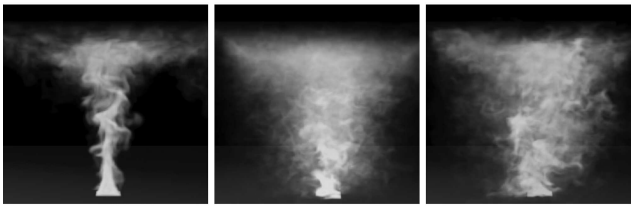

(b) Second Vorticity Confinement, ε/μ is: 5, 10, 20

(c) Our method, ε/μ is: 30, 120, 300

Figure 3: *Robustness comparison of three methods. No synthesis methods are used in this experiment*.

Figure 3c. This indicates that our method is more stable and robust, due to our use of the positive diffusion term to constrain the total confinement adaptively.

Figure 4 compares our method with other methods in procedural synthesis. Figure 4a is produced by our method in low resolution. This forms the main flow of the turbulence. Figure 4b shows the use of vortex particle [YKH*09] in Figure 4a to synthesize fine details. This method produces a relatively stable vector field and does not blow up. However, as spatial coherence between the particles will lead to artefacts at high vortical forces and particles directly affecting the density will over roll the flows, unrealistic turbulence may be produced as shown. Figure 4b shows the use of adaptive vorticity confinement (AVC) [HWPW11] in Figure 4a to synthesize fine details. The main limitation of AVC is that it is an unstable method as it integrates velocity dimension into the confinement term. As can be seen from this example that the smoke is over-dispersed in the middle part due to the excessive energy. Figure 4c shows the use of our new method in Figure 4a to synthesize highly turbulent details, where the vector field is generated with $\epsilon_{high}/\mu_{high} = 600$. We can see that realistic fine details are added to the turbulence without noise.

Figure 5 shows various effects produced by changing the four parameters, ϵ_{low} and μ_{low} in low resolution and ϵ_{high} and μ_{high} in high resolution. In order for the vortex details to be more visible, we use ray-casting to render these images. For each pair of images, we show how a single parameter affects the appearance of the turbulence, while keeping the other three parameters unchanged. We first set it to a low value and then a high value. Figures 4a and 4b show that by increasing the value of ϵ_{low}, we increase the size of the vorticals. Hence, the size of turbulence becomes larger. Figures 4c and 4d show that by increasing the value of μ_{low}, we reduce the lifetime of the vorticals. As a result, the vorticals disappear much more quickly and the size of the turbulence appears to be smaller. Figures 4e–4h show similar comparisons but for sub-grid details in the high-resolution step. In summary, the parameters in low resolution control the shape of flows, while the parameters in high resolution control the small-scale details and the dispersive degree.

Figure 6 demonstrates that our method can be used to produce thin smoke. We model this thin smoke to form the words 'Computer Graphics Forum' and let it pass through the cylinders. The animation sequence show that our method can produce dispersive thin smoke without artefacts, even at high $\epsilon_{high}/\mu_{high}$ values.

Table 1 compares the frame rate of our method with other energy injection methods, AVC [HWPW11] (our earlier method) and vortex particle [YKH*09]. We can see that our new method has a similar,

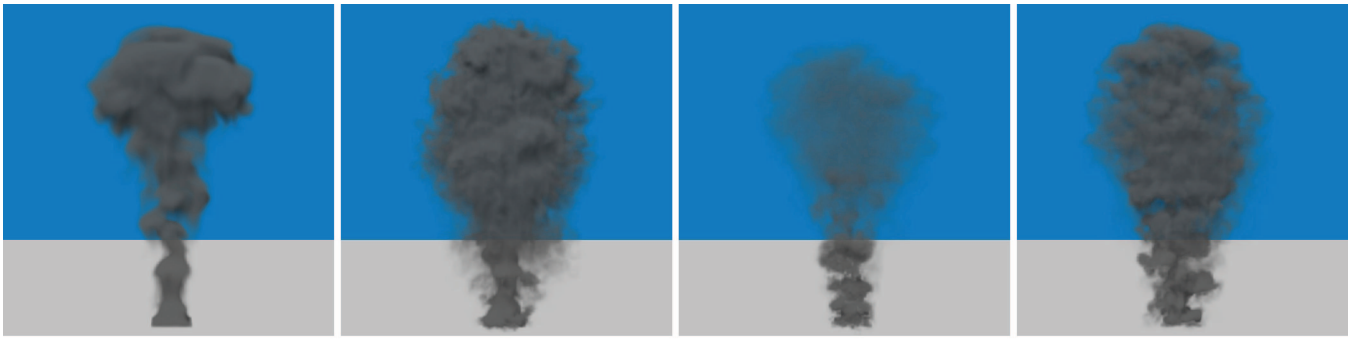

(a) Our method on a coarse grid (b) Vortex Particle method applied to (a) (c) Adaptive Vorticity Confinement applied to (a) (d) Our method applied to (a) with $\varepsilon_{high} = 12.0$

Figure 4: *Comparison of different procedural synthesis methods. All diagrams are produced with a* $128 \times 128 \times 128$ *simulation based on a* $64 \times 64 \times 64$ *coarse grid. (a) Our method on a coarse grid (without adding high-resolution details). (b) High vorticity maximum vortex particle method* [YKH*09] applied to (a). *(c) High-strength AVC* [HWPW11] applied to (a). *(d) Our method applied to (a) with* $\epsilon_{high} = 12.0$, $\epsilon_{high}/\mu_{high} = 600$.

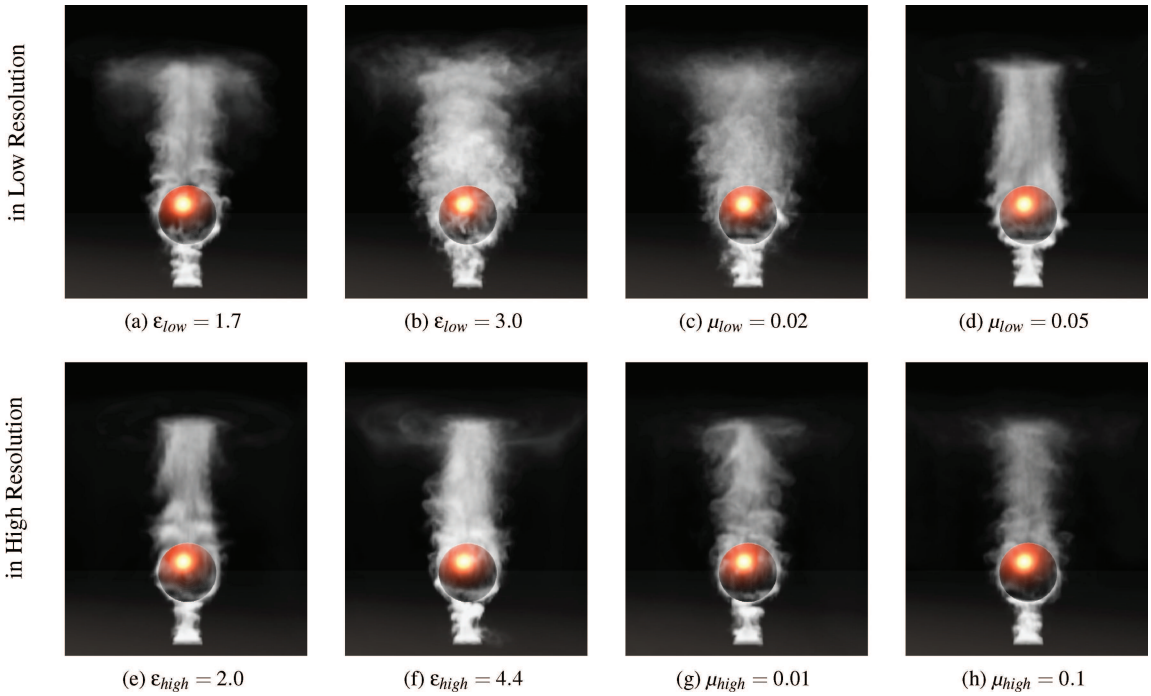

(a) $\varepsilon_{low} = 1.7$ (b) $\varepsilon_{low} = 3.0$ (c) $\mu_{low} = 0.02$ (d) $\mu_{low} = 0.05$

(e) $\varepsilon_{high} = 2.0$ (f) $\varepsilon_{high} = 4.4$ (g) $\mu_{high} = 0.01$ (h) $\mu_{high} = 0.1$

Figure 5: *Varying the four parameters. The top row shows the low-resolution step for generating the main flow, while the bottom row shows the high-resolution step for generating sub-grid details. (a) and (b) compare the effects of setting different* ϵ_{low}, *while keeping the other three parameters the same. Likewise, (c) and (d) compare the effects of* μ_{low}, *(e) and (f) compare the effects of* ϵ_{high} *and (g) and (h) compare the effects of* μ_{high}. *We use ray-casting in this experiment so that the effects can be more visible.*

but slightly lower frame rate than AVC and vortex particle. As compared with AVC, the computation time of both methods depends on the coarse resolution as well as the target resolution. Our method has a slightly lower frame rate due to the added positive diffusion term. The computation time of vortex particle depends only on the coarse resolution and the number of particles used in the target resolution. This experiment shows that although our method produces more robust and realistic turbulence, its computational cost is only slightly higher than those of AVC and vortex particle. This can be considered as a trade-off between visual quality and performance.

As a summary, our method has several advantages. First, it is robust and explicitly conserves momentum. Second, it is easy to implement, due to its simplicity. Third, the control of the resulting turbulence is more intuitive, through four parameters with two in the low resolution and two in the high resolution. Fourth, we have

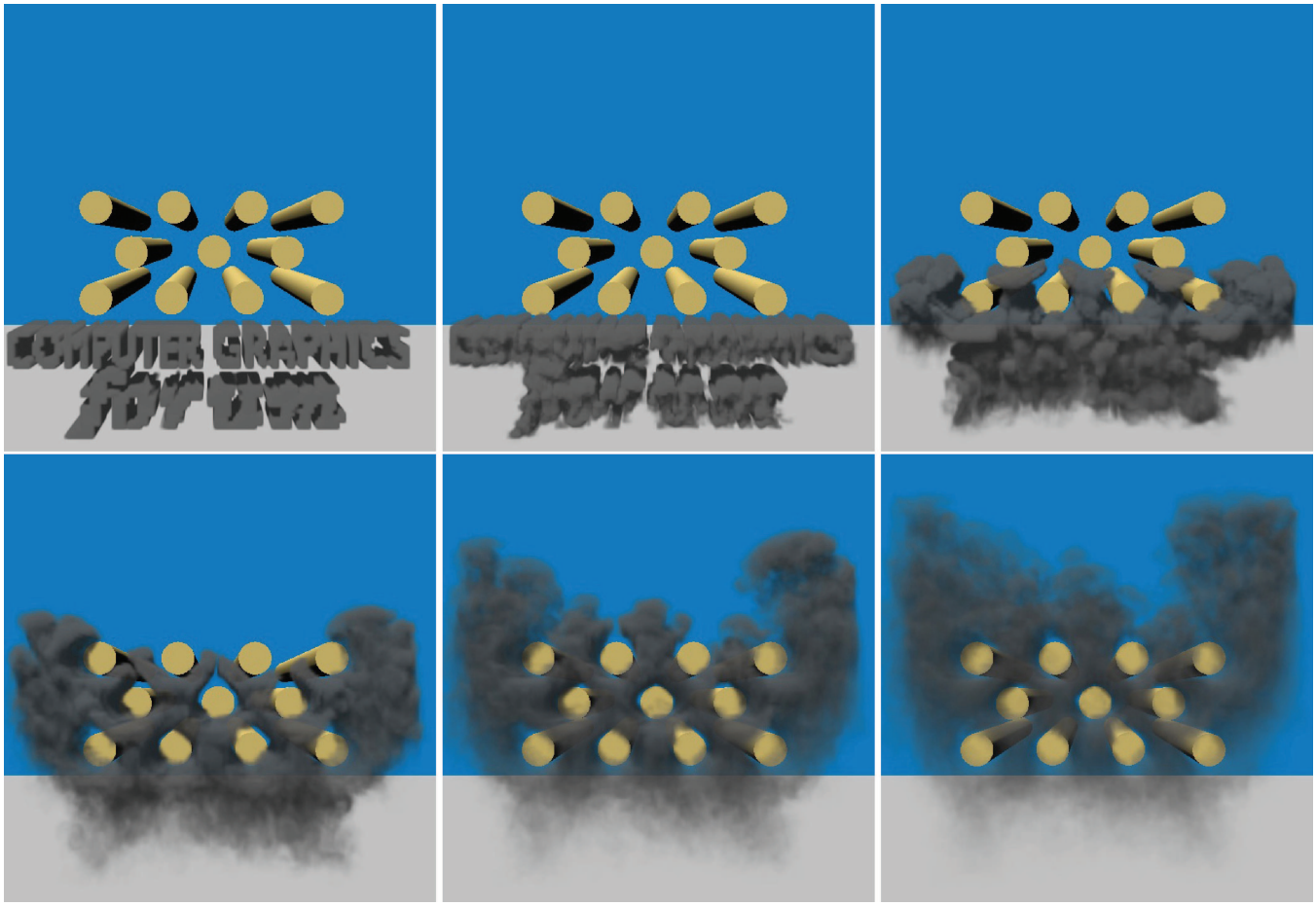

Figure 6: *Smoke forming the words 'Computer Graphics Forum' and passing through some obstacles. It is a* $128 \times 128 \times 128$ *simulation (with* $\epsilon_{low} = 1.4$, $\mu_{low} = 0.024$, $\epsilon_{high} = 7.0$ *and* $\mu_{high} = 0.016$*) based on a* $64 \times 64 \times 64$ *coarse grid, running at 37.7 frames per second.*

Table 1. *Comparison of three turbulence methods on frame rates: our method, AVC [HWPW11] and Vortex Particle [YKH*09].*

Turbulence method	**Coarse res.**	**Target res.**	**With/Without rendering** (fps)
Our method	64^3	128^3	37.7 / 52.9
He *et al.* [HWPW11]	64^3	128^3	41.3 / 56.8
Yoon *et al.* [YKH*09]	64^3	128^3	42.2 / 58.0
Our method	128^3	256^3	6.5 / 7.0
He *et al.* [HWPW11]	128^3	256^3	7.6 / 8.2
Yoon *et al.* [YKH*09]	128^3	256^3	8.4 / 9.0

demonstrated through a number of experiments that our method produces more stable and realistic highly turbulent flows. However, our method suffers from one drawback. Since we have modified the original formulation of the positive diffusion term to balance the negative diffusion term, the modified positive term can no longer produce the normal diffusion. Consequently, our modified formulation cannot generate viscous flows as the smooth effect cannot be produced anymore.

5. Conclusion and Future Work

In this paper, we have presented a turbulence method that is based on the RVC2 method. Its objective is to synthesize highly turbulent and high-quality smoke simulation. Our RVC2 is robust enough to achieve highly turbulence flows. It exactly conserves momentum and allows more intuitive control of the turbulence. We have demonstrated that our method is more suitable in synthesizing highly turbulent sub-grid details without artefacts. Our approach is general and applicable to a wide variety of smoke phenomena as demonstrated. Experimental results show that our approach can achieve high-resolution turbulence smoke in real time.

As a future work, we have noticed that guided-based fluid simulation [NCZ*09, HMK11, YCZ11] is attracting a lot of attention in recent years. Unlike previous works that focus on large-scale behaviours [TMPS03, MTPS04], we are currently investigating on how to improve the controllability of our method

to produce small-scale details according to the guidance of either an image or an object.

Acknowledgements

We would like to thank John Steinhoff for some useful discussions and for explaining some issues related to his Vorticity Confinement and Second Vorticity Confinement methods. We would also like to thank the anonymous reviewers for the insightful and constructive comments/suggestions on our paper. The work described in this paper was partially supported by a GRF grant from the Research Grants Council of Hong Kong (RGC Reference Number: CityU 116010) and a SRG grant from City University of Hong Kong (Project Number: 7002664).

References

[Bri08] Bridson R.: *Fluid Simulation for Computer Graphics*. A K Peters, Elsevier Science B.V., Amsterdam, France, 2008.

[Cos08] Costes M.: Analysis of the second vorticity confinement scheme. *Aerospace Science and Technology 12*, 3 (2008), 203–213.

[CZY11] Chen F., Zhao Y., Yuan Z.: Langevin particle: A self-adaptive lagrangian primitive for flow simulation enhancement. *Computer Graphics Forum 30*, 2 (2011), 435–444.

[FSJ01] Fedkiw R., Stam J., Jensen H. W.: Visual simulation of smoke. In *Proceedings of ACM SIGGRAPH'01* (Los Angeles, California, USA, 2001), pp. 15–22.

[FWD*02] Fan M., Wenren Y., Dietz W., Xiao M., Steinhoff J.: Computing blunt body flows on coarse grids using vorticity confinement. *Journal of Fluids Engineering 124*, 4 (2002), 876–885.

[HMK11] Huang R., Melek Z., Keyser J.: Preview-based sampling for controlling gaseous simulations. In *Proceedings of ACM SCA'11* (Vancouver, British Columbia, Canada, 2011), pp. 177–186.

[HWPW11] He S., Wong H.-C., Pang W.-M., Wong U.-H.: Real-time smoke simulation with improved turbulence by spatial adaptive vorticity confinement. *Computer Animation and Virtual Worlds 22*, 2–3 (2011), 107–114.

[KLLR07] Kim B., Liu Y., Llamas I., Rossignac J.: Advections with significantly reduced dissipation and diffusion. *IEEE Transaction on Visualization and Computer Graphics 13* (January 2007), 135–144.

[KTJG08] Kim T., Thürey N., James D., Gross M.: Wavelet turbulence for fluid simulation. *ACM Transactions on Graphics 27* (August 2008), 50:1–50:6.

[LAF11] Lentine M., Aanjaneya M., Fedkiw R.: Mass and momentum conservation for fluid simulation. In *Proceedings of ACM SCA'11* (Vancouver, British Columbia, Canada, 2011), pp. 91–100.

[LM91] Le H., Moin P.: An improvement of fractional step methods for the incompressible navier-stokes equations. *Journal of Computational Physics 92*, 2 (1991), 369–379.

[MTPS04] Mcnamara A., Treuille A., Popović Z., Stam J.: Fluid control using the adjoint method. *ACM Transactions on Graphics 23*, 3 (August 2004), 449–456.

[NCZ*09] Nielsen M. B., Christensen B. B., Zafar N. B., Roble D., Museth K.: Guiding of smoke animations through variational coupling of simulations at different resolutions. In *Proceedings of ACM SCA'09* (New Orleans, Louisiana, USA, 2009), pp. 217–226.

[NSCL08] Narain R., Sewall J., Carlson M., Lin M. C.: Fast animation of turbulence using energy transport and procedural synthesis. *ACM Transactions on Graphics 27* (December 2008), 166:1–166:8.

[PTC*10] Pfaff T., Thuerey N., Cohen J., Tariq S., Gross M.: Scalable fluid simulation using anisotropic turbulence particles. *ACM Transactions on Graphics 29* (December 2010), 174:1–174:8.

[PTSG09] Pfaff T., Thuerey N., Selle A., Gross M.: Synthetic turbulence using artificial boundary layers. *ACM Transactions on Graphics 28* (December 2009), 121:1–121:10.

[Rob04] Robinson M.: Application of vorticity confinement to inviscid missile force and moment prediction. In *Proceedings of AIAA 42nd Aerospace Sciences Meeting and Exhibit* (Reno, Nevada, USA, 2004), pp. 717–728.

[SB08] Schechter H., Bridson R.: Evolving sub-grid turbulence for smoke animation. In *Proceedings of ACM SCA'08* (Dublin, Ireland, 2008), pp. 1–7.

[SC10] Steinhoff J., Chitta S.: Long distance wave computation using nonlinear solitary waves. *Journal of Computational and Applied Mathematics 234* (July 2010), 1826–1833.

[SFK*08] Selle A., Fedkiw R., Kim B., Liu Y., Rossignac J.: An unconditionally stable maccormack method. *Journal of Scientific Computing 35* (June 2008), 350–371.

[SFWD03] Steinhoff J., Fan M., Wang L., Dietz W.: Convection of concentrated vortices and passive scalars as solitary waves. *Journal of Scientific Computing 19* (December 2003), 457–478.

[SRF05] Selle A., Rasmussen N., Fedkiw R.: A vortex particle method for smoke, water and explosions. *ACM Transactions on Graphics 24* (July 2005), 910–914.

[Sta99] Stam J.: Stable fluids. In *Proceedings of ACM SIGGRAPH'99* (Los Angeles, California, USA, 1999), pp. 121–128.

[SU94] Steinhoff J., Underhill D.: Modification of the Eular equations for "vorticity confinement": Applicaiton to the computation of interacting vortex rings. *Physics of Fluids 6* (1994), 2738–2744.

[TMPS03] Treuille A., Mcnamara A., Popović Z., Stam J.: Keyframe control of smoke simulations. *ACM Transactions on Graphics 22*, 3 (July 2003), 716–723.

[YCZ11] Yuan Z., Chen F., Zhao Y.: Pattern-guided smoke animation with lagrangian coherent structure. *ACM Transactions on Graphics 30* (December 2011), 136:1–136:8.

[YKH*09] Yoon J.-C., Kam H. R., Hong J.-M., Kang S. J., Kim C.-H.: Procedural synthesis using vortex particle method for fluid simulation. *Computer Graphics Forum 28*, 7 (2009), 1853–1859.

[ZB05] Zhu Y., Bridson R.: Animating sand as a fluid. *ACM Transactions on Graphics 24* (July 2005), 965–972.